NATURAL NANOFLUID CONVECTION IN RECTANGULAR CAVITIES WITH VARIABLE ASPECT RATIOS AND PROTUBERANT HEAT SOURCE HEIGHTS

Paulo Mohallem Guimarães, pauloguimaraes@unifei.edu.br
Alex Pereira da Silva, alexamdv@uifei.edu.br
Mahyara Meirelles Ribeiro, mahyararibeiro@unifei.edu.br
Mário Vitor Arantes Lima, mariovitorlima@hotmail.com
Universidade Federal de Itajubá, Campus de Itabira
Genésio José Menon, genesiomenon@unifei.edu.br
Universidade Federal de Itajubá, Campus de Itajubá

Abstract. *This work investigates a natural convection in a square enclosure with a protuberant heat source. It is a laminar and non-steady regime. The finite element method is used to approximate solutions. Linear quadrilateral elements are employed to spatially discretize the domain. Several validations are carried out with numerical and experimental results. Water-based nanofluids have Copper, Alumina and Titanium oxide as its nanoparticles, separately. This work has two parts. The first part consists of lateral vertical cold walls that have variable heights and they are referred to fins, which could be considered to be part of the cooling system to refrigerate electrical transformers, for example. Ten heights are studied for these cold walls. Rayleigh number ranges from 10^4 to 10^6 and the volume fraction from 0 to 0.016, totaling 9 suspension concentrations. By combining all geometrical and physical. The second part consists of geometries with variable aspect ratio and variable heat source height and two lateral vertical cold wall heights. Just three volume concentrations are studied: 0, 0.01 and 0.015. Just part of the temperature and velocity behavior is shown here. The concentrations are chosen to be very small, since they are in agreement with the correlations used for thermal viscosity and thermal conductivity. In a general view, nanofluids proved to smoothly enhance heat transfer as the concentration increases for the range adopted. However, nanoparticle material plays an important role on heat transfer.*

Keywords: *Natural convection, nanofluid, heat source*

1. NOMENCLATURE

FH	Fin height
h	Heat transfer coefficient
k_{nf}	Nanofluid thermal conductivity
L	Characteristic length
Nu	Nusselt number
P	Dimensionless pressure
p	Dimensional pressure
Pr	Prandtl number
q''	Dimensionless heat flux
Ra	Rayleigh number
Ri	Richardson number
T	Dimensional temperature
t	Dimensional time
u	Dimensional velocity on x-direction
v	Dimensional velocity on y-direction
U and V	Dimensionless velocities in the X and Y directions, respectively
u and v	Dimensional velocities in the x and y directions, respectively

Greek symbols

α_{nf}	Balancing diffusion or nanofluid thermal diffusivity
Δ	Increment
θ	Dimensionless temperature
μ_{nf}	Nanofluid dynamic viscosity
ν	Kinematics viscosity
ρ_{nf}	Nanofluid density
$(\rho\beta)_{nf}$	Nanofluid thermal expansion
$(\rho C_p)_{nf}$	Nanofluid heat capacitance
$\varnothing$	Nanoparticle concentration
τ	Dimensionless time

Subscripts

c, h	Cold and hot surfaces, respectively
hs	heat source
f	Pure fluid
nf	Nanofluid
p	Particle

2. INTRODUCTION

Nanofluids have been scenery of quite a number of publications for the past decade due to its importance. Wen et al. (2009) presented a critical and extensive review of nanofluids for heat transfer applications. They came to the conclusion that the scientific understanding is still limited, since that many challenges are still alive which are the formulation, practical application, controlled particle size and morphology for heat transfer applications. There are some controversies in literature that may be due to uncertainties on the content of nanofluids, not to mention the solid and fluid phases. They said that not only thermal conductivity, but also other properties such as viscosity and wettability, must be seriously considered in future research. Problems with buoyancy induced flow play an important role in a variety of engineering systems due to their applications in electronic cooling, heat exchangers, etc. Ostrach (1998) made a review on these applications. Since low thermal conductivity of conventional fluids, for instance water and oils, impairs a better heat transfer performance and is a constraint of equipment compactness, an innovative technique to help enhance heat transfer, and hence decrease the size of equipment, is the use of nanoparticles in the base fluid. Such suspension composed by a base-fluid and nanoparticles was firstly named nanofluid by Choi (1995). Some numerical and experimental works on nanofluids concern thermal conductivity (Kang et al. (2006), convective heat transfer (Maiga et al.(2005), Abu-Nada (2008), boiling heat transfer and natural convection (Xuan and Li (2000). One can find a detailed review, as also mentioned in Oztop and Abu-Nada (2008), in Putra et al.(2003), Wang et al.(2006), Xuan and Li (2000), Trisaksri and Wongwises (2007), Daungthongsuk and Wongwises(2007), and Wang and Mujumdar (2007).

Aminossadati and Ghasemi (2009) studied natural convection in a square cavity with a heat source placed at the bottom insulated surface. Nanofluid was composed of water-based fluid and Copper, Silver, Alumina and Titanium oxide as for its solid particles. The authors used the nanofluid thermal conductivity for spherical nanoparticles according to Maxwell (1904) and which was also cited by other researchers such as Ho et al. (2008) and Oztop and Abu-Nada (2008) . The effective dynamic viscosity was given by Brinkman (1952). Aminossadati and Ghasemi (2009) used the volume control method as for the numerical method and the Simple algorithm to handle the pressure-velocity coupling. A 60x60 uniform grid was found to meet grid independency and CPU requirements. They studied the influence on heat transfer of volume fraction that ranged from 0 to 0.20, Rayleigh number (Ra) from 10^3 and 10^6, and heat source size from 0.2 to 0.8, for Copper, Silver, Alumina, and Titanium dioxide nanoparticles. They found that Cu and Ag nanoparticles provided the highest cooling performance, where for low Ra, the addition of 20% of these solid particles resulted in 42.8% reduction of heat source maximum temperature. Öğüt (2009) studied numerically the heat transfer by natural convection in an inclined square enclosure with a constant flux heater placed on the left vertical wall. All walls were thermally isolated, but the right vertical one, which was cooled. The heat source length was taken as 0.25, 0.50, and 1.0 (whole wall). Ra ranged from 10^4 to 10^6. The work presented the effect of volume concentration (0 to 0.2) for Copper, Silver, Copper oxide, Alumina and Titanium dioxide. As for the numerical method, polynomial-based differential quadrature (PDQ) was applied. According to the author, PDQ produces accurate numerical results, small number of grid points and, thus, requires small CPU time. The effective thermal conductivity adopted was the one proposed by Yu and Choi (2003), which is a modified version of Maxwell equation for a solid-liquid mixture that includes the effect of a liquid nanolayer on the surface of a nanoparticle. He found that the presence of nanoparticles caused substantial increase in heat transfer rate. The behavior of the average Nu was nearly linear with the volume fraction. Heat transfer rate started to decrease for smaller inclination angles as source length ranged from 0.25 to 1.0. The maximum and minimum Nu's were localized at inclinations 30^o and 90^o, respectively. Oztop and Abu-Nada (2008) conducted a study in which there was a heater under uniform temperature in an rectangular enclosure. The heater was placed on the left vertical wall. The opposite vertical wall was cooled, being that the remaining walls were isolated. The enclosure aspect ratio and also the heater size and position on the wall were investigated. The governing equations were approximated by the finite volume approach (Patankar(1980) and Versteeg and Malalasekera). The existing nanoparticles were Copper, Alumina and Titanium dioxide for a water-based nanofluid. In general, the use of nanofluids and also the increasing volume fraction increased Nu. The effect of the heater size depended mainly on the kind of nanofluid being used. For rectangular enclosures, heat transfer was more pronounced for vertically elongated enclosures. Tiwari and Das (2007) investigated the convection behavior inside a two-sided lid-driven differentially heated cavity filled with nanofluids. The vertical moving walls were isothermal and the remaining ones isolated. Results for Richardson number (*Ri*) ranging from 0.1 to 10 were presented. The transport equations were numerically approximated by using the finite volume technique and the SIMPLE algorithm. Water was used as the base-fluid and mixed with copper nanoparticles in some concentrations, such as 0.0%, 8%, 16%, and 20%. The effective viscosity was the one presented by Brinkman (1952) and the effective density and heat capacitance as the ones found in Xuan and Li (2000). The effective thermal conductivity of fluid was determined by the one of Maxwell-Garnett's model for spherical-particle suspension. They presented an extensive number of graphics containing streamlines and isotherms. It was observed that nanoparticles were able to change the flow pattern from natural to forced convection regime. When the walls had ascending movement, Nu was reduced compared to the other cases from the work. For $Ri < 1$, which features forced convection, with walls moving in opposite directions, Nu enhanced significantly regardless which side moved upwards. Gosselin and Da Silva (2004) performed a study on the maximization importance of thermal performance of nanofluid flow when adequate constraints are concerned. Their main objective was to examine the heat transfer on a plate from which heat was removed by nanofluid flowing on it. The mathematical model used was the one proposed by Hamilton and Crosser (1962), Xuan and Roetzel (2000) and Brinkman (1952). An analysis of the empirical shape parameter was carried out in function of volume concentration. They showed that as long as an appropriate constraint is used, heat transfer can be optimized in terms of volume fraction. By constraining the power dissipated by friction, an optimal volume fraction can be achieved by balancing low pumping power requirement and the need for an enhanced heat transfer rate.

The objective of this work is to perform an analysis on laminar natural convective heat transfer in a square enclosure with an internal heat source. This whole set is built to resemble, approximately, a transversal section of an electrical transformer with lateral solid fins as its cooling external system. In order to roughly simulate a fin attached to the enclosure, a cold wall with variable height is located on both vertical sides of the enclosure. In the first part, 9 heights are studied for Rayleigh numbers (*Ra*) equal to 10^3, 10^4, 10^5, 10^6 and Prandtl number (*Pr*) 6.2 (pure water). Copper (*Cu*), Alumina (Al_2O_3) and Titanium dioxide (TiO_2) are used as nanoparticles to form the nanofluids. Nine volume fractions (Ø) are considered: 0 (pure water), 0.002, 0.004, 0.006, 0.008, 0.01, 0.012, 0.014, and 0.016. The second part, some geometric parameters are varied: two cold wall heights, three heat source heights, and two cavity widths. Three volume fractions (*Ø*) are considered: 0 (pure water), 0.01 and 0.015. Copper (*Cu*) is used as the nanoparticle. *Ra* numbers are 10^4, 10^5, and 10^6 and Prandtl number (*Pr*) 6.2 (pure water). The finite element method is used to approximate the conservation equations, together with the Petrov-Galerkin technique to treat the convective terms and the penalty formulation to deal with the pressure terms. A linear quadrilateral element is used to discretize the spatial domain. The code is thoroughly validated by comparing present results with the ones found in numerical and experimental works from literature. In order to verify the mesh independency, two meshes are analyzed. Afterwards, results for temperature and velocity behavior will be shown. Also, plots of Nusselt number versus fin height, volume concentration, etc, are presented.

3. MATHEMATICAL FORMULATION

Figure 1 shows a square enclosure whose outer surfaces are considered thermally isolated (hachured part) and cooled at uniform temperature T_c (non-hachured part). As for the internal surfaces, they belong to an internal heat source whose surfaces deliver a uniform and constant heat flux *q"* to the inner fluid domain. The inner fluid domain is composed by a water-based nanofluid. The nanoparticles that belong to the suspensions studied are Copper (Cu), Alumina (Al_2O_3) and Titanium dioxide (TiO_2) whose thermophysical properties are shown in Table 1. This work does not consider oil, which is used in most electrical transformers. This may be considered in future works. On the right side of Fig.1, one may find the respective surfaces and their dimensionless lengths. For the first part, the geometrical parameters are *FH* (fin height) = 0.1, 0.2, 0.3, 0.4, 0.5, 0.6, 0.7, 0.8, 0.9 and 1.0 (whole vertical wall), *CH* (core height) = 0.5 and *W* (width) = 0.5. For the second part, the geometrical parameters are *FH* (fin height) = 0.5 and 1.0 (whole vertical wall), *CH* (core height) = 0.25, 0.5, 0.75 and *W* (width) = 0.5 and 0.75. This wok also intends to study the interaction among the fin heights and the heat source cooling for various Rayleigh numbers. The Rayleigh number is the product of buoyancy and viscosity forces within a fluid and Prandtl number, which describes the relationship between momentum diffusivity and thermal diffusivity. Throughout this work, half of the geometry will be studied, since there is a symmetry line at *x=0*. This saves CPU time and, hence, enables a more refined mesh on the surfaces of interest over which the Nusselt number is calculated.

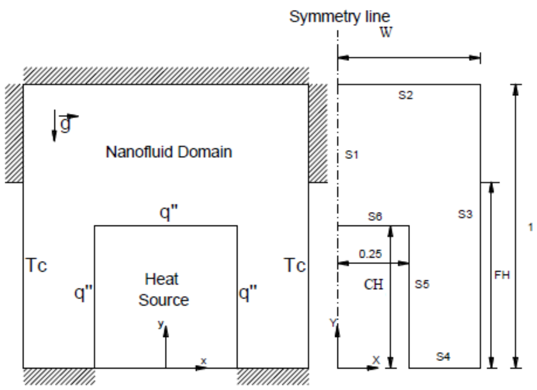

$$S_1 \Rightarrow U=0, \frac{\partial \theta}{\partial X}=0 \,(simmetry); \; S_2 \Rightarrow U=V=0, \frac{\partial \theta}{\partial Y}=0 \,(isolated\ wall)$$

$$S_3 \Rightarrow \begin{cases} U=V=0, \frac{\partial \theta}{\partial X}=0 \,(hachured\ part \Rightarrow isolated\ wall) \\ U=V=0, \theta=0 \,(non-hachured\ part \Rightarrow cooled\ wall) \end{cases}$$

$$S_3 \Rightarrow \begin{cases} U=V=0, \frac{\partial \theta}{\partial X}=0 \,(hachured\ part \Rightarrow isolated\ wall) \\ U=V=0, \theta=0 \,(non-hachured\ part \Rightarrow cooled\ wall) \end{cases} \quad S_4 \Rightarrow U=V=0, \frac{\partial \theta}{\partial Y}=0 \,(isolated\ wall)$$

$$S_5 \Rightarrow U=V=0, \frac{\partial \theta}{\partial X}=-1 \,(wall\ with\ heat\ flux); \; S_6 \Rightarrow U=V=0, \frac{\partial \theta}{\partial Y}=-1 \,(wall\ with\ heat\ flux)$$

Figure 1. Geometry and boundary conditions.

The governing equations are the conservation equations of mass, momentum and energy for a two-dimensional laminar and non-steady natural convection in terms of nanofluid physical properties.

The effective density ρ_{nf} and the thermal diffusivity α_{nf} of the nanofluid are given as:

$$\rho_{nf} = (1-\phi)\rho_f + \phi \rho_p, \qquad \alpha_{nf} = k_{nf} \big/ \left(\rho C_p\right)_{nf} \tag{1}$$

The nanoparticles, which will be considered in this study, are Copper (*Cu*), Alumina (Al_2O_3), and Titanium dioxide (TiO_2). The base fluid is water with Prandtl number (*Pr*) equal to 6.2. Table 1 gives the thermophysical properties of water and nanoparticles according to Oztop and Abu-Nada (2008):

Table 1 – Thermophysical properties of fluid and nanoparticles

Physical properties	Water	*Cu*	Al_2O_3	TiO_3
Cp (J/kgK)	4179	385	765	686.2
ρ (kg/m^3)	997.1	8933	3970	4250
K (W/mK)	0.613	400	40	30.7
β x 10^{-5} (1/K)	21	1.67	0.85	0.9

The heat capacitance $(\rho C_p)_{nf}$ and the thermal expansion $(\rho\beta)_{nf}$ of the nanofluid are written as:

$$\left(\rho C_p\right)_{nf} = (1-\phi)\left(\rho C_p\right)_f + \phi\left(\rho C_p\right)_p , \qquad (\rho\beta)_{nf} = (1-\phi)(\rho\beta)_f + \phi(\rho\beta)_p \tag{2}$$

The effective dynamic viscosity μ_{nf} of the nanofluid (Brinkman (1952)) is:

$$\mu_{nf} = \frac{\mu_f}{(1-\phi)^{2.5}} \tag{3}$$

The thermal conductivity k_{nf} for spherical particles and based on Maxwell –Garnett's model (1904), is:

$$k_{nf} = k_f \left[\frac{\left(k_p + 2k_f\right) - 2\phi\left(k_f - k_p\right)}{\left(k_p + 2k_f\right) + \phi\left(k_f - k_p\right)} \right] \tag{4}$$

where k_p is the thermal conductivity addressed to nanoparticles (Copper, Alumina and Titanium Oxide), and k_f is the thermal conductivity addressed to pure fluid (water). The Maxwell-Garnett's model has been cited by other authors such as Aminossadati and Ghasemi (2009), Ho et al. (2008) and Oztop and Abu-Nada (2008).

Since this is a dimensionless study, the conservation equations should be re-written in terms of dimensionless parameters, which are as follows:

$$X = \frac{x}{L}; Y = \frac{y}{L}; U = \frac{uL}{\alpha_f}; V = \frac{vL}{\alpha_f}; P = \frac{pL^2}{\rho_{nf}\alpha_f^2}; \tau = \frac{t}{\left(L^2/\alpha_f\right)}; \theta = \frac{(T - T_c)}{(\Delta T)}; Ra = \frac{g\beta_f L^3 \Delta T}{\nu_f\,\alpha_f}; \Delta T = \frac{q'' L}{k_f}; Pr = \frac{\nu_f}{\alpha_f} \tag{5}$$

For that being so, the dimensionless governing equations of mass, momentum and energy conservation are:

$$\frac{\partial U}{\partial X} + \frac{\partial V}{\partial Y} = 0 \tag{6}$$

$$\frac{\partial U}{\partial \tau} + U\frac{\partial U}{\partial X} + V\frac{\partial U}{\partial Y} = -\frac{\partial P}{\partial X} + \frac{\mu_{nf}}{\rho_{nf}\alpha_f}\left(\frac{\partial^2 U}{\partial X^2} + \frac{\partial^2 U}{\partial Y^2}\right) \tag{7}$$

$$\frac{\partial V}{\partial \tau} + U\frac{\partial V}{\partial X} + V\frac{\partial V}{\partial Y} = -\frac{\partial P}{\partial Y} + \frac{\mu_{nf}}{\rho_{nf}\alpha_f}\left(\frac{\partial^2 V}{\partial x^2} + \frac{\partial^2 V}{\partial y^2}\right) + \frac{(\rho\beta)_{nf}}{\rho_{nf}\beta_f} Ra\,Pr\,\theta \tag{8}$$

$$\frac{\partial \theta}{\partial \tau} + U\frac{\partial \theta}{\partial X} + V\frac{\partial \theta}{\partial Y} = \frac{\alpha_{nf}}{\alpha_f}\left(\frac{\partial^2 \theta}{\partial X^2} + \frac{\partial^2 \theta}{\partial Y^2}\right) \tag{9}$$

The local Nusselt number and the average Nusselt number are, respectively:

$$Nu_{hs}^*(X,Y) = \left.\frac{1}{\theta(X,Y)}\right|_{hs}, \quad Nu_{hs}(X,Y) = \frac{1}{S}\int_{hs} Nu_{hs}^* \tag{10}$$

4. NUMERICAL PROCEDURE AND CODE VALIDATION

Equations (6) to (9) are approximated by the finite element method with Petrov-Galerkin weighting on the convective terms and the pressure terms are approximated by a penalty technique with the penalty parameter equal to 10^9. These techniques will be omitted here for a space matter. They can be found in a variety of literature, for instance, Heinrich and Pepper (1999). The numerical method is implemented by using a Fortran program. The code is thoroughly validated. Just part of it is shown. Table 2 consists of a comparison with a benchmark problem in which a square differentially heated cavity is studied where the vertical wall temperatures are uniform and equal to 0 (cold wall) and 1 (hot wall). compares the average Nusselt number along the hot wall, the maximum velocities in the X and Y directions and their respective positions at Y and X axes, for Ra equal to 10^3, 10^4, 10^5 and 10^6. However, only comparisons for Ra equal to 10^3 and 10^6 and shown. Air is the work fluid with Pr = 0.7. Excellent agreement is achieved.

Table 2. Comparison table for square differentially heated cavity with wall temperatures 0 and 1.

Ra		Present	Khanafer et al. (2003)	Barakos and Mitsoulis (1994)	Markatos &Pe-ricleous(1984)	De Vahl Davis (1984)	Fusegi et al. (1991)
	Nu	1.1208	1.118	1.114	1.108	1.118	1.105
10^3	*Umax* (at *y/H*)	0.1379 (0.8120)	0.137 (0.812)	0.153 (0.806)	- (0.832)	0.136 (0.813)	0.132 (0.833)
	Vmax (at *x/H*)	0.1400 (0.1780)	0.139 (0.173)	0.155 (0.181)	- (0.168)	0.138 (0.178)	0.131 (0.200)
	Nu	8.8363	8.826	8.806	8.754	8.799	9.012
10^6	*Umax* (at *y/H*)	0.0760 (0.8500)	0.077 (0.854)	0.077 (0.859)	- (0.872)	0.079 (0.850)	0.084 (0.856)
	Vmax (at *x/H*)	0.2620 (0.038)	0.262 (0.039)	0.262 (0.039)	- (0.038)	0.262 (0.038)	0.259 (0.033)

One more validation is presented in Table 3 and it is related to nanofluid behavior. The problem is taken from Aminossadati and Ghasemi (2009). The problem consists of a square cavity with a heat source with length *B* placed on the middle of the bottom surface. All walls are cooled at temperature zero, but the remaining bottom surface is isolated. The base fluid is water with *Pr* = 6.2 and the nanoparticles used are Copper, Alumina and Titanium Oxide. Results for average Nusselt number and maximum temperature on the heat source are obtained for *Ra* equal 10^3, 10^4(not shown), 10^5(not shown) and 10^6. In general, an excellent agreement is observed.

Table 3. Comparison for the case with a heater on the bottom of a square cavity with Ø = 0.1, *B* = 0.4 and *Pr* = 6.2.

		Nu_m		T_{max}	
		Present	Aminossadati and Ghasemi (2009)	Present	Aminossadati and Ghasemi (2009)
Ra=10^3	*Cu*	5.4681 *(0.30%)*	5.451	0.205 *(0.00%)*	0.205
	Al_2O_3	5.4075 *(0.30%)*	5.391	0.207 *(0.00%)*	0.207
	TiO_2	5.2058 *(0.32%)*	5.189	0.215 *(0.00%)*	0.215
Ra=10^6	*Cu*	13.5222 *(2.53%)*	13.864	0.109 *(1.84%)*	0.107
	Al_2O_3	13.4093 *(1.89%)*	13.663	0.110 *(1.82%)*	0.108
	TiO_2	13.1595 *(1.95%)*	13.416	0.113 *(1.77%)*	0.111

5. RESULTS AND DISCUSSION

A mesh independebcy srudy was carried out ranging grids with 20000 to 40000 elements. Errors ranged from 0% to 0.1%. In the present section 5, Figure 2 and Table 4 regard part one and other figures and tables concern part two.

Figure 2 depicts the average Nusselt on the heat source surface in function of the nanoparticle concentrations for *FH* = 1, *Ra* from 10^3 to 10^6, also contrasting the effects of the three nanoparticles (Copper (*Cu*), Alumina (Al_2O_3) and Titanium dioxide (TiO_2)). This is a graphic where one can clearly note the effects of concentration and material by keeping *Ra* and *FH* fixed. However, it is worth mentioning the importance of verifying *Nu* ranges reached here by looking at its order on the graphic axes. In a general way, *Nu* gets higher as concentration increases. For all cases, the Copper water-based nanofluid is the one that features the highest deviation of average Nusselt number on the heat source (Nu_{hs}) (highest curve inclination). It is important to point out that the thermal conductivity of Cooper is about ten times the ones of Alumina (Al_2O_3) and Titanium dioxide (TiO_2). Other *FH*'s present the same behavior.

Table 4 presents the module values of deviations for Nu_{hs} and θ_{max} on the heat source for *Cu* nanofluids. The highest deviation occur for low *Ra*, that is, the role of nanofluids regarding cooling of the heat source is more significant when the ratio of floatability and viscosity forces and the product of thermal and dynamic diffusivities is smaller. In this case, that is, low *Ra*, the temperature order is lower and, hence, the nanofluid becomes more efficient. The deviation order of Nuhs with *Ra* = 10^3 and *FH* = 0.5, is 3% and 4.5% for Ø = 0.01 and Ø = 0.016, respectively. This same order is valid for *Ra* = 10^3 and *FH* = 0.7 and 1. When high *Ra*'s are concerned, the temperature values are also high, thus, the nanofluid performance tends to become weaker. In other words, since the correlations for thermal conductivity and viscosity of the nanofluid considered in this work depends solely on the small nanoparticle concentration, which means that they do not vary with temperature and the nanoparticle diameter, these two properties do not change as *Ra* increases when a case is taken individually with fixed concentration. Hence, these two properties do no change when the heat source temperature increases. For that being so, the role of the nanofluid conductivity given by the presence of nanoparticles has more effect for lower temperature values. This is a very interesting result, indeed. It is worth pointing out that all this work is carried out for very low nanoparticle concentration of the order of 1%. The authors strongly suggest other studies using higher concentrations where thermal conductivity and dynamic viscosity correlations take into account not only concentration but also temperature and particle diameter.

The second part, that is, CH = 0.25, 0.5, 0.75, FH = 0.5, 1.0, W = 0.5, 1.0, $Ø$ = 0, 0.01, 0.015, $Ra = 10^4$, 10^5, 10^6, for Copper only, is presented in Table 5. Since we are dealing in this part with a small order of Nusselt number variations regarding nanoparticle concentration by keeping other parameters constant, it is interesting to show data in the form of a

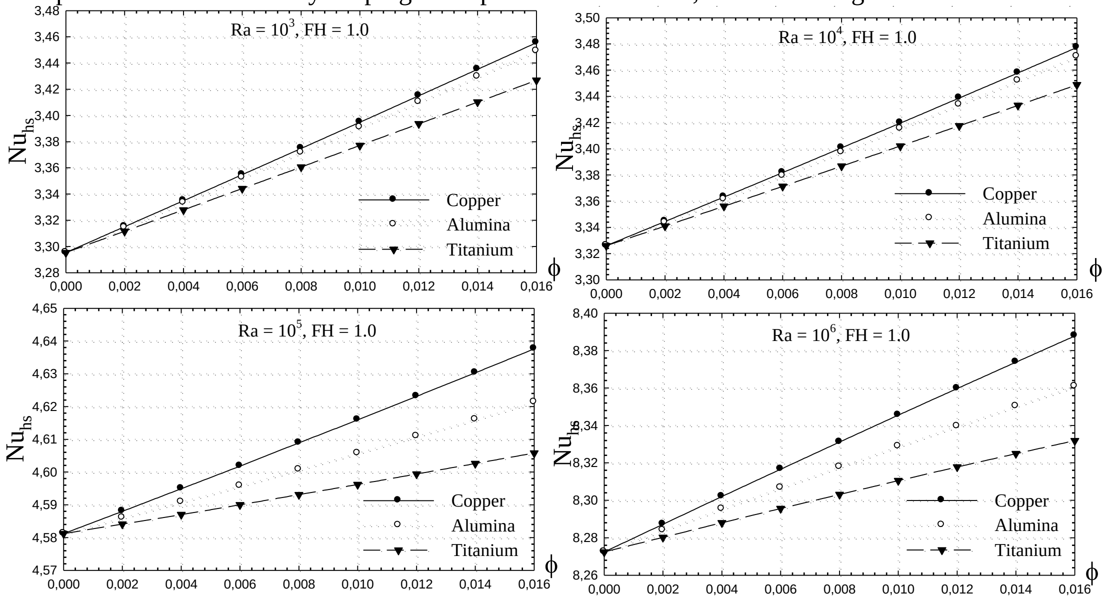

Figure 2 – Nusselt versus concentration for FH = 1 and $Ra = 10^3$ a 10^6.

Table 4. Module values of deviations for Nu_{hs} and $Ø_{max}$ on the heat source for Cu nanofluids.

		Nusselt Number					Heat Source Temperature				
FH	*Ra*	Water	*Ø*=1%	|Dev.|	*Ø*=1.6%	|Dev.|	Water	*Ø*=1%	|Dev.|	*Ø*=1.6%	|Dev.|
0.5	10^3	2.6688	2.75	3.01	2.80	4.84	0.3647	0.36	2.91	0.3479	4.61
	10^4	2.7248	2.80	2.72	2.85	4.40	0.3555	0.35	2.62	0.3407	4.16
	10^5	3.7157	3.75	0.97	3.77	1.56	0.2584	0.26	0.93	0.2545	1.51
	10^6	6.3134	6.38	1.03	6.42	1.64	0.1528	0.15	1.05	0.1503	1.64
0.7	10^3	3.1154	3.21	3.02	3.27	4.86	0.3217	0.31	2.92	0.3068	4.63
	10^4	3.1565	3.24	2.79	3.30	4.50	0.3144	0.31	2.64	0.3013	4.17
	10^5	4.3092	4.35	0.85	4.37	1.37	0.2266	0.23	0.79	0.2236	1.32
	10^6	7.5598	7.63	0.98	7.68	1.55	0.1295	0.13	1.08	0.1273	1.70
1.0	10^3	3.2953	3.40	3.02	3.46	4.86	0.3104	0.30	2.93	0.2960	4.64
	10^4	3.3260	3.42	2.82	3.48	4.55	0.3043	0.30	2.66	0.2915	4.21
	10^5	4.5812	4.62	0.76	4.64	1.23	0.2181	0.22	0.69	0.2157	1.10
	10^6	8.2724	8.35	0.89	8.39	1.40	0.1191	0.12	0.92	0.1174	1.43

table. Therefore, Table 5 presents the Nusselt numbers and the maximum temperature for all cases, where W, FH and CH are geometric parameters referring to width, cold wall height and the heat source height, respectively. The deviations shown in the last column refer to the Nusselt number variations for the cases with nanofluid from the ones of pure water. One can note that, again, the most significant deviations are found for small Rayleigh numbers, that is, $Ra = 10^4$. For example, for $W = 0.5$, FH = 0.5, CH = 0.25, and $Ra = 10^4$, the deviations are 2.71% and 4.10%, for Ø = 1% and 1.5 %, respectively. For the same geometry just mentioned with $Ra = 10^6$, the corresponding deviations are 0.8% for $Ø$ = 1% and 1.2% for $Ø$ = 1.5%. This pattern repeats when $W = 0.75$. The nanoparticle presence seems to be more effective when Ra decreases. The aspect ratio also affects the heat transfer. One can compare the cases from the left hand side of the table, W = 0.5, with their respective ones from the right hand side, W = 0.75. By doing so, one studies the influence of letting the cold wall surface be more distant from the heat source surface, and therefore, more space for the fluid to flow between those two surfaces. For $Ra = 10^4$ and 10^5, the geometries with W = 0.5 present Nu_{hs} higher than the ones with W = 0.75. On the other hand, Nu_{hs} for $Ra = 10^6$ and W = 0.75 are higher than those for $W = 0.5$. As Ra increases in this analysis, the regime turns to be more convective and hence allowing more cold fluid flow in the space between the heat source and the cold wall. When Ra is small, the more conductive regime is favored when those two surfaces are closer.

7. CONCLUSIONS

In the present work an analysis was carried out to see the influence of nanoparticles in a base fluid (water) on the behavior of heat transfer inside a square cavity with a protuberant heat source placed inside it on the bottom surface.

Table 5. Isotherms, Nusselt numbers and θmax for the second part.

W	FH	CH	Ra	φ%	Nu_{hs}	Nu_c	θ_{MAX}	Dev(%)
0,5	0,5	0,25 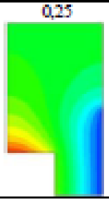	10^4	0	3,666	0,979	0,3811	0,00
				1	3,765	0,95	0,3701	2,71
				1,5	3,816	0,936	0,3646	4,10
			10^5	0	4,6	0,967	0,3156	0,00
				1	4,676	0,939	0,3103	1,66
				1,5	4,715	0,926	0,3076	2,50
			10^6	0	7,409	0,968	0,2113	0,00
				1	7,469	0,939	0,2091	0,80
				1,5	7,498	0,925	0,208	1,20
		0.5 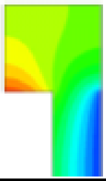	10^4	0	3,017	1,457	0,2723	0,00
				1	3,104	1,415	0,2647	2,89
				1,5	3,149	1,394	0,2611	4,35
			10^5	0	3,493	1,443	0,2317	0,00
				1	3,554	1,402	0,228	1,75
				1,5	3,586	1,382	0,2261	2,66
			10^6	0	5,709	1,437	0,1384	0,00
				1	5,757	1,395	0,1372	0,85
				1,5	5,781	1,375	0,1367	1,27
		0,75 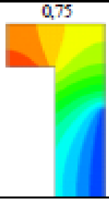	10^4	0	2,218	1,932	0,2984	0,00
				1	2,281	1,876	0,2905	2,84
				1,5	2,313	1,848	0,2866	4,28
			10^5	0	2,621	1,916	0,2404	0,00
				1	2,665	1,861	0,237	1,68
				1,5	2,688	1,834	0,2353	2,54
			10^6	0	4,189	1,91	0,1419	0,00
				1	4,232	1,854	0,1407	1,03
				1,5	4,253	1,827	0,1401	1,53
	1	0,25 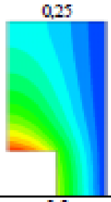	10^4	0	4,051	0,501	0,3124	0,00
				1	4,156	0,486	0,304	2,59
				1,5	4,21	0,479	0,2998	3,93
			10^5	0	5,448	0,501	0,2179	0,00
				1	5,535	0,486	0,2155	1,59
				1,5	5,578	0,479	0,2144	2,39
			10^6	0	8,62	0,501	0,1389	0,00
				1	8,681	0,486	0,1378	0,70
				1,5	8,711	0,479	0,1373	1,05
		0,5 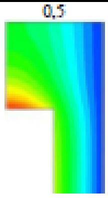	10^4	0	3,92	0,751	0,3507	0,00
				1	4,032	0,729	0,3401	2,85
				1,5	4,089	0,718	0,3349	4,31
			10^5	0	4,679	0,75	0,2878	0,00
				1	4,766	0,728	0,2832	1,85
				1,5	4,81	0,718	0,2809	2,79
			10^6	0	7,58	0,75	0,2005	0,00
				1	7,626	0,728	0,1984	0,60
				1,5	7,648	0,718	0,1974	0,90
		0,75 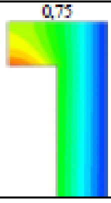	10^4	0	3,623	1,002	0,2517	0,00
				1	3,73	0,972	0,2444	2,96
				1,5	3,785	0,958	0,2408	4,46
			10^5	0	3,996	1,001	0,2359	0,00
				1	4,075	0,972	0,2306	1,96
				1,5	4,116	0,958	0,2279	2,98
			10^6	0	6,675	1	0,1512	0,00
				1	6,71	0,971	0,1501	0,51
				1,5	6,726	0,957	0,1496	0,76

W	FH	CH	Ra	φ%	Nu_{hs}	Nu_c	θ_{MAX}	Dev(%)
0,75	0,5	0,25 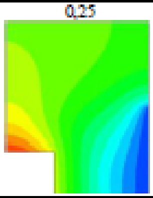	10^4	0	2,5611	0,973	0,3588	0,00
				1	2,6009	0,9448	0,3539	1,55
				1,5	2,6214	0,9311	0,3514	2,35
			10^5	0	4,1065	0,9722	0,2121	0,00
				1	4,1472	0,9436	0,2103	0,99
				1,5	4,1674	0,9297	0,2095	1,48
			10^6	0	6,8904	0,9767	0,1286	0,00
				1	6,9513	0,948	0,1272	0,88
				1,5	6,9813	0,934	0,1266	1,32
		0.5 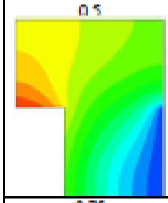	10^4	0	2,0014	1,4576	0,4111	0,00
				1	2,0342	1,4153	0,4063	1,64
				1,5	2,0512	1,3948	0,4038	2,49
			10^5	0	3,2637	1,456	0,2354	0,00
				1	3,2943	1,4132	0,2336	0,94
				1,5	3,3094	1,3924	0,2327	1,40
			10^6	0	5,4379	1,4595	0,1327	0,00
				1	5,4914	1,4167	0,1319	0,98
				1,5	5,5179	1,3959	0,1315	1,47
		0.75 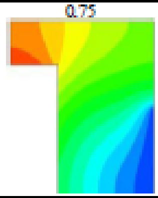	10^4	0	1,6039	1,9393	0,4405	0,00
				1	1,6294	1,8829	0,4359	1,59
				1,5	1,6425	1,8555	0,4335	2,41
			10^5	0	2,5364	1,9379	0,2511	0,00
				1	2,5652	1,8811	0,2492	1,14
				1,5	2,5795	1,8535	0,2483	1,70
			10^6	0	4,0762	1,9383	0,1394	0,00
				1	4,1208	1,8817	0,1386	1,09
				1,5	4,143	1,8542	0,1382	1,64
	1	0.25 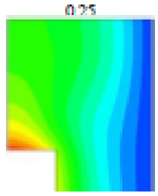	10^4	0	3,0738	0,5004	0,3597	0,00
				1	3,1111	0,4858	0,3554	1,21
				1,5	3,1303	0,4787	0,3531	1,84
			10^5	0	5,1249	0,5005	0,2083	0,00
				1	5,1736	0,4858	0,2069	0,95
				1,5	5,1977	0,4787	0,2063	1,42
			10^6	0	8,4717	0,5005	0,1261	0,00
				1	8,5508	0,4859	0,125	0,93
				1,5	8,5899	0,4788	0,1245	1,40
		0,5 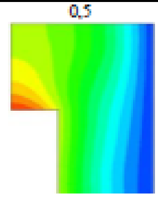	10^4	0	2,5269	0,7501	0,4134	0,00
				1	2,5637	0,7282	0,4064	1,46
				1,5	2,5831	0,7175	0,4028	2,22
			10^5	0	4,4373	0,75	0,2349	0,00
				1	4,4673	0,728	0,2337	0,68
				1,5	4,4818	0,7174	0,2331	1,00
			10^6	0	7,5614	0,7501	0,1395	0,00
				1	7,6359	0,7282	0,1379	0,99
				1,5	7,6726	0,7175	0,1372	1,47
		0,75 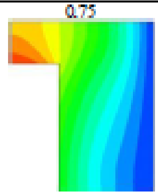	10^4	0	2,1934	1	0,379	0,00
				1	2,2256	0,9707	0,3754	1,47
				1,5	2,2424	0,9565	0,3735	2,23
			10^5	0	3,8165	0,9995	0,2039	0,00
				1	3,8442	0,9702	0,2025	0,73
				1,5	3,8577	0,956	0,2019	1,08
			10^6	0	6,5939	0,9992	0,121	0,00
				1	6,6532	0,97	0,1197	0,90
				1,5	6,6825	0,9558	0,1191	1,34

The Nusselt number variation was not significant when volume concentration was ranged. Nevertheless, the material played an important role when volume concentration was kept constant and a fixed Ra and a fixed fin height. The authors strongly encourage this same study with other correlations for thermophysical proportions where higher concentrations will be possible.

6. ACKNOWLEDGEMENTS

The authors thank CNPq and FAPEMIG for the financial support.

7. REFERENCES

Abu-Nada E., 2008, "Application of nanofluids for heat transfer enhancements of separated flows encountered in a backward-facing step", Int. J. Heat Fluid Flow 29, pp. 242-249.

Aminossadati S.M., Ghasemi B., 2009, "Natural, convection cooling of a localized heat source at the bottom of a nanofluid-filled enclosure", European Journal of Mechanics B/Fluids, pp. 1-11.

Barakos G., Mitsoulis E., 1994, "Natural convection flow in a square cavity revisited: laminar and turbulent models with wall functions", Int. J. Num. Methods Fluids 18, pp. 695-719.

Brinkman H. C., 1952, "The viscosity of concentrated suspensions and solution, J. Chem. Phys. 20, pp. 571-581.

Choi U. S., 1995, "Enhancing thermal conductivity of fluids with nanoparticles", in: D.A. Siginer, H.P. Wang, (Eds), Developments and applications od Newtonian flows, FED 231 (66), pp. 99-105.

Daungthongsuk W., Wongwises S., 2007, “A critical review of convective heat transfer nanofluids”, Renew Sustain. Energy Rev 11, pp. 797-817.

De Val Davis G., 1962, “Natural convection of air in a square cavity, a benchmark numerical solution”, Int. J. Num. Methods Fluids 3, pp. 249-264.

FIDAP Theoretical Manual, 1990, Fluid Dynamics International, Evanston, IL, USA.

Fusegi T., Hyun J. M., Kuwahara K., Farouk B., 1991, “A numerical study of three-dimensional natural convection in a differentially heated cubical enclosure”, Int. J. Heat Mass Transfer 34, pp. 1543-1557.

Gosselin L., Da Silva A. K., 2004, “Combined “heat transfer and power dissipation” optimization of nanofluid flows”, Applied Physics Letters 85 (18), pp. 4160-4162.

Hamilton R. L., Crosser O. K., 1962, “Thermal conductivity of heterogeneous two-component systems”, I & EC Fundam. 1, pp. 182-191.

Heinrich J. C., Pepper D. W., 1999, Intermediate Finite Element Method, Ed. Taylor & Francis, USA.

Ho C. J., Chen M. W., Li Z. W., 2008, “Numerical simulation of natural convection of nanofluid in a square enclosure: effects due to uncertainties of viscosity and thermal conductivity”, Int. J. Heat Mass Transfer 51 (17-18), pp. 4506-4516.

Kang H. U., Kim S. H., Oh J. M., 2006, “Estimation of thermal conductivity of nanofluid using experimental effective particle volume, Exp Heat Transfer” 19, pp. 181-191.

Khanafer K., Vafai K., Lightstone M., 2003, “Buoyancy-driven heat transfer enhancement in a two-dimensional enclosure utilizing nanofluids”, Int. J. Heat Mass Transfer 46, pp. 3639-3653.

Krane R. J., Jessee J., 1983, “Some detailed field measurements for a natural convection flow in a vertical square enclosure”, Proceedings of the First ASME-JSME Thermal Engineering Joint Conference 1, pp. 323-329.

Maiga S. E. B., Palm S. J., Nguyen C. T., Roy G., Galanis N., 2005, “Heat transfer enhancement by using nanofluids in forced convection flows”, Int. J. Heat Fluid Flow 26, pp. 530-546.

Markatos N. C., Pericleous K. A., 1984, “Laminar and turbulent natural convection in an enclosed cavity”, Int. J. Heat Mass Transfer 27, pp. 772-775.

Maxwell J., A treatise on electricity and magnetism, second ed. Oxford University Press, Cambridge, UK (1904).

Öğüt E. B., 2009, “Natural convection of water-based nanofluids in an inclined enclosure with a heat source”, Int. J. of Thermal Sciences, pp. 1-11.

Ostrach S., 1998, Natural convection in enclosures, J Heat Transfer 110, pp. 1175-1190.

Oztop H. F., Abu-Nada E., 2008, “Numerical study of natural convection in partially heated rectangular enclosures filled with nanofluids, Int. J. heat Fluid Flow”, 29 (5), pp. 1326-1336.

Patankar S. V., 1980, Numerical heat transfer and fluid flow, Hemisphere Publishing Corporation, Taylor and Francis Group, New York.

Putra N., Roetzel W., Das S. K., 2003, “Natural convection of nano-fluids”, Heat Mass Transfer 39, pp. 775-784.

Tiwari R. K., Das M. K., 2007, “Heat transfer augmentation in a two-sided lid-driven differentially heated square cavity utilizing nanofluids”, 50, pp. 2002-2018.

Trisaksri V., Wongwises S., 2007, “Critical review of heat transfer characteristics of nanofluids”, Renew. Sustain. Energy Rev. 11, pp. 512-523.

Versteeg H. K., Malalasekera W., An introduction to computational fluid dynamic: The finite volume method. John Wiley & Sons Inc., New York.

Wang X.-Q, Mujumdar A. S., Yap C., 2006, “Free convection heat transfer in horizontal and vertical rectangular cavities filled with nanofluids”, Int. Heat Transfer Conference IHTC 13 Sydney, Australia.

Wang X-Q, Mujumdar A. S., 2007, “Heat transfer characteristics of nanofluids: a review”, Int. J. Therm. Sci. 46, pp. 1-19.

Wen D., Lin G., Vafaei S., Zhang K., 2009, “Review of nanofluids for heat transfer applications”, Particuology, 7, 141-150.

Xuan Y., Li Q., 2000, “Heat transfer enhancement of nanofluids”, Int. J. Heat Fluid Flow 21, pp. 58-64.

Xuan Y., Roetzel W., 2000, “Conceptions for heat transfer correlation of nanofluids”, Int. J. Heat Mass Transfer 43, pp. 3701-3707.

Yu W., Choi S.U.S., 2003, “The role of interfacial layers in the enhanced thermal conductivity of nanofluids: a renovated Maxwell model”, J. Nanoparticle Res. 5, pp. 167-171.

8. RESPONSIBILITY NOTICE

The authors are the only responsible for the printed material included in this paper.